7. ANKARA INTERNATIONAL AEROSPACE CONFERENCE **AIAC-2013-139**
11-13 September 2013 - METU, Ankara TURKEY

THRUST GENERATION OF PLUNGING AIRFOILS IN TANDEM AND BIPLANE CONFIGURATIONS

S.Banu Yucel*, Mehmet Sahin† and M.Fevzi Unal‡
Istanbul Technical University
Istanbul, Turkey

ABSTRACT

The propulsion performance of NACA0012 airfoils undergoing harmonic plunging motion in tandem and biplane arrangements is numerically and experimentally investigated. An unstructured finite volume solver based on Arbitrary Lagrangian-Eulerian formulation is utilized in order to solve the incompressible unsteady Navier-Stokes equations. Four different tandem and four different biplane configurations are considered. Various instantaneous and time-averaged aerodynamic parameters including the lift and thrust coefficients, vorticity contours are calculated. As a reference, the single airfoil case corresponding to the deflected jet phenomenon reported Jones and Platzer (2009) is also studied. In these simulations, the Reynolds number is chosen to be 252 and the reduced frequency of plunging motion ($k = 2\pi fc/U_\infty$) and the plunge amplitude non-dimensionalized with respect to chord are 12.3 and 0.12 respectively. In the experimental phase of the study plunging single airfoil in the thrust mode is investigated using Digital Particle Image Velocimetry (DPIV) at $Re = 2,000$, $5,000$ and $10,000$. Experiments also revealed various types of interaction of flow fields from airfoils in tandem arrangement at $Re = 2,000$.

INTRODUCTION

Studying flapping wing aerodynamics is essential in understanding the complicated nature of bird and insect flight mechanisms and thus in being able to drive inspiration from nature in designing the related engineering products. Micro Air Vehicles (MAVs) are one of the most common applications of flapping wing aerodynamics with potential civil and military applications such as the terrestrial and indoor monitoring. The early studies on the lift and thrust generation via flapping is made independently in 1909 and 1912, by Knoller and Betz respectively as explained in the study of [Jones et al., 1998]. According to that study, Knoller and Betz were the first to indicate that an effective angle of attack is generated on a wing due to flapping, leading to a normal force vector with both lift and thrust components. Later on in 1922, Katzmayr made the first experimental verification of the Knoller-Betz effect by placing a fixed airfoil into a sinusoidally oscillating wind stream and measured thrust. Two years after Katzmayr, Birnbaum identified the conditions for thrust generation and he recommended the use of a sinusoidally plunging wing as an alternative to the conventional propeller. [Jones et al., 1998] studied the effect of non-dimensional plunge velocity (V_p) on force generation. From the flow visualization results they observed that at small V_p values, similar to stationary airfoils, sinusoidally plunging airfoils generate drag. The drag is reduced and eventually the thrust is generated when V_p is further increased. In the same study, flow patterns are obtained also numerically, by using an inviscid, unsteady panel code that employs a nonlinear wake model. According to this study, a non-symmetric, deflected wake pattern, indicating both an average thrust and an average lift production, occur when V_p is on the order of 1.5. [Tuncer and Platzer, 1996] investigated the thrust production on a single NACA0012 flapping airfoil and a flapping-stationary airfoil pair in tandem by employing a multi block Navier-Stokes solver for unsteady flow

*Gra. in Department of Astronautical Engineering, Email: yucelsa@itu.edu.tr
†Assoc.Prof. in Department of Astronautical Engineering, Email: msahin@itu.edu.tr
‡Prof. in Department of Aeronautical Engineering, Email: munal@itu.edu.tr

fields. According to their numerical results, a substantial enhancement is achieved for the flapping-stationary tandem configuration. It is claimed that the propulsive efficiency is strongly related with reduced frequency and flapping amplitude. The propulsive efficiency of single airfoil was computed to be over 70%, at flapping amplitude of $0.4c$ and a reduced frequency of 0.1. However, in the tandem case where the airfoils are two chord lengths apart from each other, the propulsive efficiency increased more than 40% at a reduced frequency of 0.75 and flapping amplitude of $0.2c$. [Jones and Platzer, 2001] stated that by making use of the interference effect between a flapping forewing and a non-flapping hindwing, an efficient flapping foil propeller can be developed. An oscillatory flow on the stationary hindwing due to the vortical energy generated by the flapping forewing can be converted into an additional thrust by means of the Katzmayr effect. In the numerical study of [Broering et al., 2010] two airfoils in tandem configuration was investigated at Reynolds number of 10^4. The flow field was modeled by solving the incompressible Navier-Stokes equations. In order to simulate the flapping motion an overlapping moving grid method was utilized. The main parameters of the study were the Strouhal number and the phase difference between the fore and hindwings to understand their effects on the force generation. Three different phase angles 0^o, 90^o and 180^o, were employed. They stated that for the forewing, the lift, thrust and resultant force increased when compared with a single airfoil. On the other hand, for the hindwing lift and resultant force decreased whereas thrust increased for 0 degree phase difference and decreased for 90 and 180 degrees phase differences. Moreover, when compared to the two isolated single wing case, for the combined wings at 0^o phase difference, the magnitude of resultant force changed considerably but its direction inclined forward and thus indicated decreased lift and increased thrust. At 90 and 180 degrees phase difference cases, resultant force, lift and thrust were all decreased. [Jones and Platzer, 2001] studied several wing configurations such as single, tandem and biplane. For their study, a test model was built which allowed all the aforementioned combinations, including two forewings either in pure or combined pitching/plunging motion with two stationary hindwings. According to their unsteady panel code analysis, they showed that biplane configuration was rather promising. In the same study, it was also stated that for the propulsion system of MAVs, adequate thrust can be produced for hovering flight with the biplane configuration. [Jones et al., 2005] carried out a study on the improvement and flight testing of a radio-controlled MAV with flapping wing propulsion system, which was composed of a low aspect ratio fixed-wing with a counter phase flapping trailing pair of higher aspect ratio wings. Like the flight in ground effect, a mechanically and aerodynamically stable platform is provided by the symmetric flapping wing couple, which increases efficiency and suppresses stall over the main wing by flow entrainment. According to their results the static thrust figure of merit for the aforementioned device was 60% higher than propellers with a similar scale and disk loading. [Kaya et al., 2009] studied the parameter optimization of biplane airfoil configuration in order to get maximum thrust and/or propulsive efficiency. A parallel flow solver on moving and deforming overset grids was used for resolving the unsteady and viscous flow fields around airfoils in pitching and plunging motion. For a range of flapping frequencies, sinusoidal pitch and plunge amplitudes and phase difference between the airfoils are optimized. Their results showed that biplane airfoil configuration produced about 25% more thrust than a single airfoil within $0.17 < St < 0.25$ but above this range thrust is decreased dramatically compared to the single airfoil. Recently [Tay et al., 2013] investigated the interaction between a plunging wing and a stationary tail in a combined experimental and numerical study at Re=5,000 and 10,000. They showed that the angle of attack of the tail and the flapping wing-tail distance have significant effects on the performance of the tandem wings; increasing the angle of attack of the tail increases its lift and drag simultaneously, but the percentage increase is higher for the lift than the drag.The study herein deals with the interacting flows from and thrust generation by NACA0012 airfoils in tandem and biplane configurations. The aim is to reveal various mechanisms of interaction of vortices from the airfoils leading to enhanced thrust production due to presence of a nearby airfoil. Towards this aim a numerical study at Re=252 is carried out. Experimental investigation using DPIV at $Re = 2,000$, $5,000$ and $10,000$ augments the findings of the numerical phase of the study.

METHOD

An unstructured finite volume solver based on an Arbitrary Lagrangian-Eulerian formulation is utilized in order to solve the incompressible unsteady Navier-Stokes equations. The numerical method uses a side-centered arrangement of the primitive variables that does not require any $ad\text{-}hoc$ modifications in order to enhance pressure coupling. In the present work, special attention is given to satisfy the continuity equation exactly within each element and the summation of the continuity equations can be exactly reduced to the domain boundary, which is important for the global mass conservation. The mesh deformation within the fluid domain is achieved by using an algebraic approach based on algebraic function at each time level while avoiding re-meshing in order to enhance numerical robustness. Special attention is also given to satisfy the discrete geometric conservation law (DGCL). For the parallel solution of resulting large-scale algebraic equations in a fully coupled form, a matrix factorization is introduced similar to that of the projection method for the whole system and two-cycle of BoomerAMG solver is used for the scaled discrete Laplacian provided by the HYPRE library which we access through the PETSc library.

In the experimental phase of the study, two Plexiglas NACA0012 wing models with $100mm$ chord and $300mm$ wingspan are used in a large scale water channel available at the Trisonic Laboratory of the Faculty of Aeronautics and Astronautics. The cross-sectional dimensions of the main test section of the channel are $1,010mm \times 790mm$. The channel has a settling reservoir and honeycomb-screen arrangements in order to maintain low turbulence intensity which is less than 1%. The maximum velocity of the water channel at $710mm$ water level is $0.13m/s$. The plunging motion is performed with two Kollmorgen/Danaher Motion AKM33E servo motors and their gear systems. The flow is illuminated by a dual cavity Nd:Yag laser and the water is seeded with silver coated hollow glass spheres of $10\mu m$ mean diameter. The flow images are captured by two 10 bit flow sense cameras with $1,600 \times 1,200$ pixels resolution and $30Hz$ frame rate.

RESULTS

In the numerical study the Reynolds number based on the airfoil chord length c and the free stream velocity U_∞ is taken to be 252 as in the work of [Jones and Platzer, 2009]. The vertical plunge motion of the NACA0012 airfoil with a frequency of f and a phase angle of ϕ is given by $y(t) = hsin(2\pi ft + \phi)$ where h is the non-dimensional plunge amplitude with respect to the airfoil chord length. The non-dimensional reduced frequency k is defined to be $2\pi fc/U_\infty$. Numerically investigated multiple wing configurations at $h = 0.12$ and $k = 12.3$ are given below:

$$
Tandem\begin{cases} Tandem, & \text{Moving forewing + stationary hindwing} \\ Shifted\,Tandem, & \text{Moving forewing (shifted down } 0.06c\text{) + stationary hindwing} \\ Tandem\ Synchronous, & \text{Both moving in same phase} \\ Tandem\ Asynchronous, & \text{Both moving in counter phase} \end{cases}
$$

$$
Biplane\begin{cases} Biplane, & \text{Moving upper wing + stationary lower wing} \\ Biplane\ Synchronous, & \text{Both moving in same phase} \\ Biplane\ Asynchronous, & \text{Both moving in counter phase} \\ Biplane\ Asynchronous\ Closer, & \text{Both moving in counter phase} \end{cases}
$$

Validation Cases of Single Airfoil in Plunging Motion

The first validation case corresponds to the experimental work of [Jones and Platzer, 2009] related with the deflected jet phenomenon. The computed vorticity contours shown in Figure 1 left column, with a phase angle of 180° indicate a non-symmetric, deflected jet very similar to that of the experiments. The current detailed studies showed that the periodic solutions highly depend on the initial conditions and to the position of the starting vortices. As an example, the calculations with a phase angle of 90° indicate a symmetrical jet. These numerical results are verified by performing spatial and temporal convergence studies. Therefore, without knowing the initial conditions it is not possible to reproduce the positions of the experimental vortices shown in Figure 1, on top of left column. Consequently, the calculations revealed that a strong hysteresis effect is present in the calculations and there are multiple periodic solutions. The second validation case corresponds to the sinusoidally plunging NACA0012 airfoil at a higher Reynolds number of 20,000. The computed vorticity contours is shown in Figure 1, on the right column and compared with the experimental result of [Lai and Platzer, 1999] and the numerical result of [Young and Lai, 2001]. It can be stated that current study is in good agreement with those studies.

Tandem Cases

In the tandem cases the instantaneous vorticity contours are shown in Figure 2. The horizontal distance between the equal chord airfoils is one chord long. For the first two, namely the Tandem and the Shifted Tandem cases, the hindwing is stationary in the wake of the forewing. Since the phase angle is zero, the wake of the forewing deflects downward before interacting with the hindwing. The counterclockwise vortices originating from the lower surface of the forewing is split almost in half by the hindwing while the clockwise vortices escape splitting and convect towards the lower side. The split counterclockwise vortex induces a clockwise vortex separation from the leading edge of the hindwing and thus produces a counterrotating vortex pair on the upper face. On the lower face a stronger counterrotating vortex pair is formed by the split counterclockwise vortex and the clockwise vortex which escapes splitting. As a result, the wake is developed as big and small counterrotating vortex pairs on upper and lower sides of the hindwing, which shoot off the centerline with their own induced velocity fields while convecting downstream. In the Shifted Tandem case, the forewing is moved 0.06c downward from the centerline. Therefore, the vortices shedding from the forewing

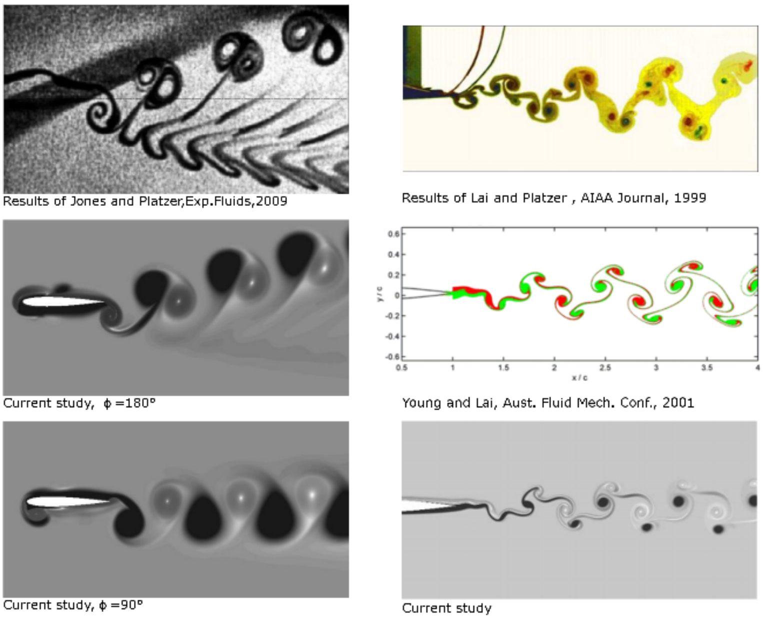

Figure 1: Comparison of the present results with several results in the literature (left column) $Re = 252$, $k = 12.3$, $h = 0.12$,(right column)$Re = 20,000$, $k = 4$, $h = 0.0125$

completely pass underneath the hindwing and form counterrotating vortex pairs and create a relatively lower pressure region on the lower hindwing surface. For the last two tandem cases, the hindwing is also moving and more complex vortex interactions occur. For the Tandem Synchronous case, during impingement of vortices with counterclockwise rotation a strong clockwise leading edge vortex is formed from the downward travelling hindwing. Therefore majority of the impinging vortex with counterclockwise rotation is directed toward the upperside of the hindwing while the clockwise vortex escapes splitting and convects downstream. Subsequent interactions of these vortices with the vorticity layers on the upper and lower surfaces and the trailing edge vortices are such that an inverse Kármán Street is formed behind the hindwing. In the Tandem Asynchronous case both positive and negative vortices split into two, interact with hindwing and then form a single wake downstream of the airfoil pair. In the last two cases, the strength of the vortices in the wake is larger in comparison with those of the previous.

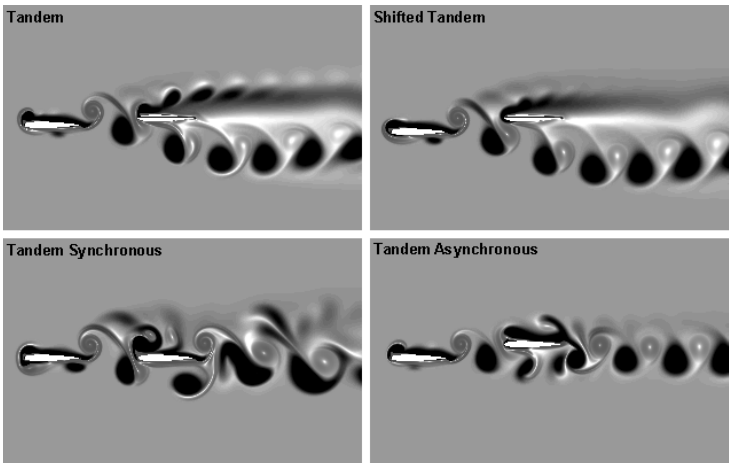

Figure 2: Instantaneous vorticity contours for tandem cases

Biplane Cases

For all biplane cases of equal chord airfoils with one chord separation distance, instantaneous vorticity contours are shown in Figure 3. In the basic Biplane case, in the upper left of the figure, the lower wing is stationary and there is not a pronounced interaction between the wakes from the airfoils. A thrust producing wake is formed in the presence of the fixed nearby airfoil. For the Biplane Synchronous case in which both airfoils plunge synchronously, two separate wakes eventually combine into one with reversed Kármán street formation far downstream, whereas in the Biplane Asynchronous case counter rotating vortex pairs originating from the upper and lower airfoils in reversed-Kármán arrangement first symmetrically shoot away from and then curve in towards the centerline. Inner vortices of the counter rotating vortex pairs feed into a large counter rotating vortex pair centered around the centerline, while those on the outer sides of the vortex couples developes into vortex pairs with reversed configuration immediately downstream. These reversed vortex couples indicate a jet flow effect and therefore a thrust. A similar interaction takes place in the Biplane Asynchronous Closer case but the length of the wake is increased. In Table1 where lift and thrust coefficients are listed for all cases it is clear that the maximum thrust enhancement is achieved in the Biplane Asynchronous Closer case.

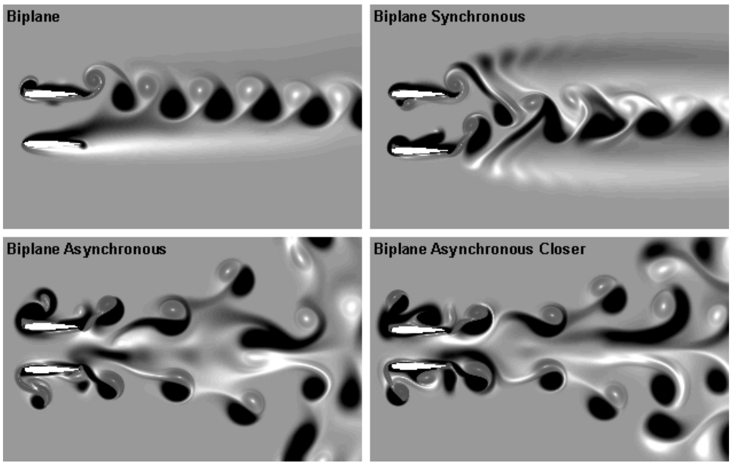

Figure 3: Instantaneous vorticity contours for biplane cases

Table 1: The mean lift and thrust coefficient values for all cases

Test cases			C_L	C_T
Single			-1.4760	0.9881
Tandem	Tandem	forewing (m)	-1.1665	0.9910
		hindwing (s)	0.0796	-0.0648
	Shifted	forewing (m)	-1.8886	1.0461
		hindwing (s)	0.3361	-0.0790
	Synchronous	forewing (m)	-3.3486	1.1948
		hindwing (m)	-1.5867	1.8775
	Asynchronous	forewing (m)	0.0640	0.8837
		hindwing (m)	-0.0769	-0.0954
Biplane	Biplane	upper wing (m)	0.7555	0.9604
		lower wing (s)	0.1525	-0.2053
	Synchronous	upper wing (m)	-5.8714	0.6887
		lower wing (m)	5.9003	0.6947
	Asynchronous	upper wing (m)	3.4718	1.6536
		lower wing (m)	-3.7362	1.6216
	Asynch. closer	upper wing (m)	3.0784	1.6981
		lower wing (m)	-3.3869	1.7742

Experimental Study

In the experimental phase of the study, firstly the single airfoil in plunging motion is studied for the verification purpose and as a step for later studies. Reynolds numbers are chosen to be $2,000$, $5,000$ and $10,000$. In accord with the earlier studies [Platzer et al., 2008] for a range of k-h value pairs the plunging airfoil is shown to result in thrust producing reversed Kármán vortex street wake in Figure 4. For comparison, all the pictures correspond to the mid position of the airfoil during plunging motion and the vorticity scale is kept constant at $Re = 5,000$ and $10,000$ whereas at $Re = 2,000$ vorticity values are multiplied by two for comparability.

Wake evolution within a period of plunging is shown in Figure 5 for the Tandem, Tandem Synchronous and Tandem Asynchronous cases at $Re = 2,000$. The top picture for all cases, i.e. $t = 0$ corresponds to the mid position. In all the cases formation of counterclockwise leading edge and clockwise trailing end vortices from the forewing during upward stroke and clockwise leading edge and counterclockwise trailing end vortices during downward stroke are apparent. In both strokes co-rotating leading and trailing end vortices merge at the trailing end of the forewing and interact with the downstream wing. In the Tandem case the merged vortices are split by the hindwing into two. For instance the merged vortex with counterclockwise rotation at $t = 0.5T$ is split into two by the hindwing at $t = 0.75T$. The upper portion starts interacting with the upper surface of the hindwing and induces a clockwise rotating vortex at its leading edge. While these counter rotating vortices interact and proceed downstream, a merged vortex with clockwise rotation formed at $t = 0$ at the trailing end of the forewing is split into two by the hindwing at $t = 0.25T$. The lower portion of the split vortex induces a counterclockwise rotating leading edge vortex and drifts downstream with it.

In the Tandem Synchronous case, the fore and hindwing are plunging synchronously. Therefore the interaction of the merged vortex originating from the trailing end of the forewing is complicated by the leading edge vortex formation during upstroke of the hindwing. In this case, virtually the entirety of the merged vortex is directed towards the reversed side of the wake by the action of the coexisting counter rotating vortex formed at the leading edge of the hindwing. This interaction leads to a reversed Kármán street with increased thrust effect.

In the Tandem Asynchronous case reversed Kármán street formation immediately behind the forewing is not promoted due to the fact that a scissoring action of the hindwing lets only a portion of the merged vortex to the reversed side of the wake. It should be noted that the numerically obtained hindwing thrust coefficient variation in Table1 at a much smaller Re number also indicates a maximum for the Tandem Synchronous case parallel to the above explained interaction.

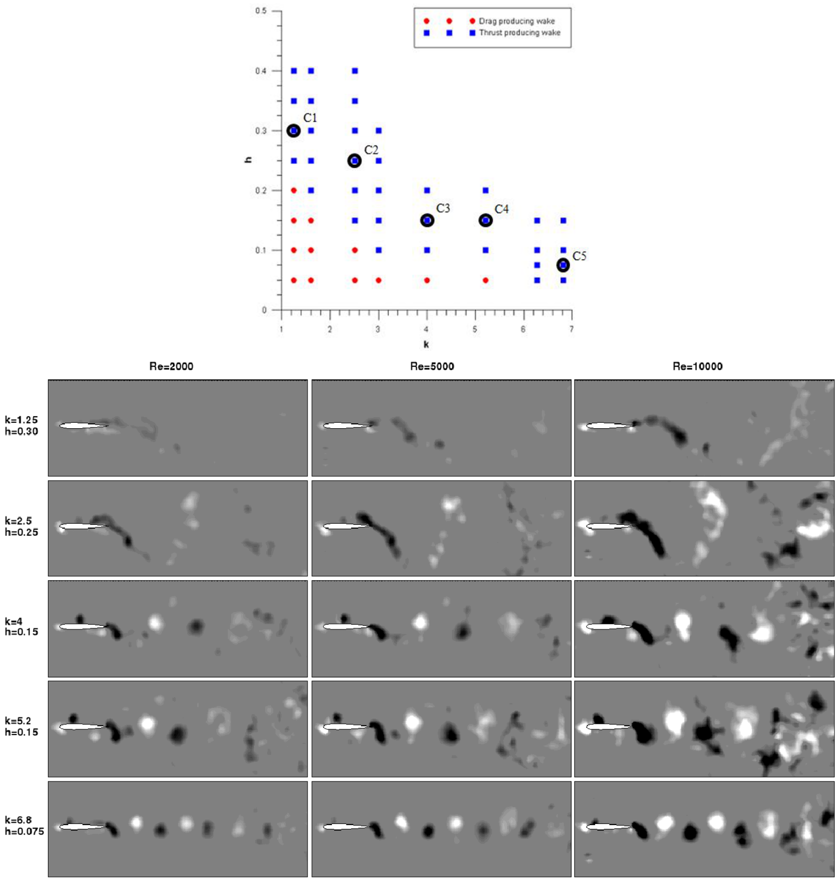

Figure 4: Instantaneous vorticity contours for cases c1, c2, c3, c4 and c5 (top to bottom) indicated in the k-h diagram, retrieved from [Percin, 2009]

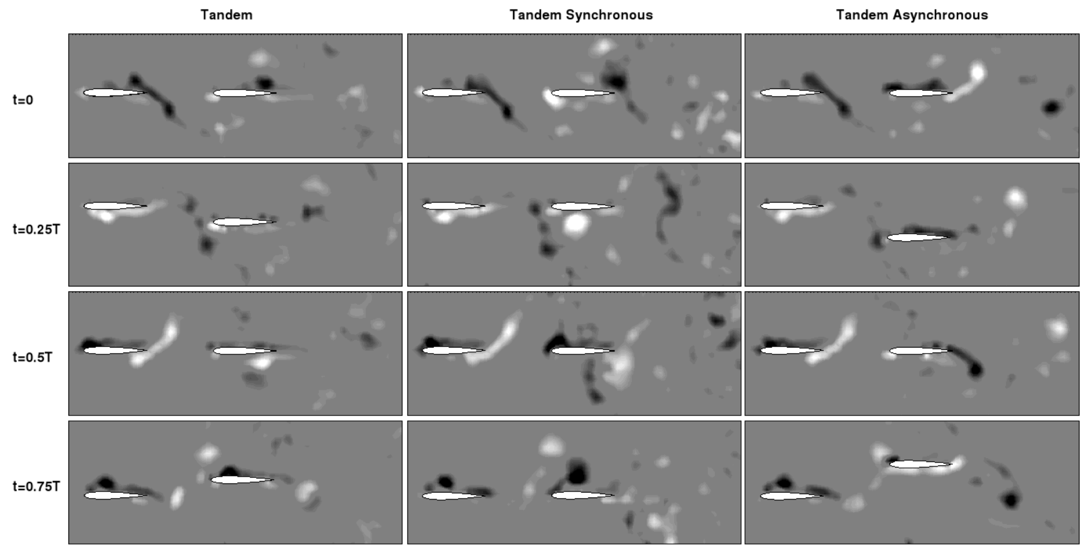

Figure 5: Wake evolution within a period of plunging motion for Re=2000 at k=2.5, h=0.25

References

Broering, T. M., Lian, Y., and Henshaw, W. (2010). Numerical Study of Two Flapping Airfoils in Tandem Configuration. Proceedings of 48th AIAA aerospace sciences meeting including the new horizons forum and aerospace exposition, AIAA 2010-0865.

Jones, K. D., Bradshaw, C. J., Papadopoulos, J., and Platzer, M. F. (2005). Bio-inspired design of flapping-wing micro air vehicles. *Aeronautical Journal*, 109(2950):385–393.

Jones, K. D., Dohring, C. M., and Platzer, M. F. (1998). Experimental and Computational Investigation of the Knoller-Betz Effect. *AIAA Journal*, 36:1240–1246.

Jones, K. D. and Platzer, M. F. (2001). On the Use of Vortex Flows for the Propulsion of Micro-Air and Sea Vehicles. Symposium on Advanced Flow Management: Part A Vortex Flows and High Angle of Attack for Military Vehicles.

Jones, K. D. and Platzer, M. F. (2009). Design and development considerations for biologically inspired flapping-wing micro air vehicles. *Experiments in Fluids*, 46(5):799–810.

Kaya, M., Tuncer, I. H., Jones, K. D., and Platzer, M. F. (2009). Optimization of Flapping Motion Parameters for Two Airfoils in a Biplane Configuration. *Journal of Aircraft*, 46:583–592.

Lai, J. C. S. and Platzer, M. F. (1999). Jet Characteristics of a Plunging Airfoil. *AIAA Journal*, 37:1529–1537.

Percin, M. (2009). Flow around a plunging airfoil in a uniform flow. Master thesis, Istanbul Technical University.

Platzer, M. F., Jones, K. D., Young, J., and Lai, J. C. S. (2008). Flapping-Wing Aerodynamics: Progress and Challenges. *AIAA Journal*, 46:2136–2149.

Tay, W. B., Percin, M., van Oudheusden, B. W., Bijl, H., Cetiner, O., and Unal, M. F. (2013). Numerical and experimental analysis of tandem flapping flight. *21st AIAA Computational Fluid Dynamics Conference, San Diego, California, USA.*

Tuncer, I. H. and Platzer, M. F. (1996). Thrust generation due to airfoil flapping. *AIAA Journal*, 34:324–331.

Young, J. and Lai, J. C. S. (2001). Frequency and Amplitude Effects in the Wake of a Plunging Airfoil. *14th Australasian Fluid Mechanics Conference Adelaide University.*